

Effect of a soft protein corona on the fibrinogen induced cellular oxidative stress of gold nanoparticles

Inga Kuschnerus, Michael Lau, Kalpeshkumar Giri, Nicholas Bedford, Joanna Biazik, Juanfang Ruan, Alfonso Garcia-Bennett

Figure S1 Surface enhanced Raman spectroscopy (SERS) spectra	page 1
Table S1 Tentative assignments of Raman bands	page 2
Figure S2 Comparison of proteomics data	page 3
Table S2 Small Angle X-ray Scattering (SAXS) and pair distance distribution function	page 4
Figure S3 Raw SAXS data	page 5
Table S3 Form factor fit of SAXS data	page 5
Figure S5 Cryo-TEM images of pure bovine serum and fibrinogen	page 6
Figure S6 DLS and zeta-potential measurements of different corona complexes	page 7
Figure S7 Additional biological TEM images	page 7
Figure S8 Flow cytometry and oxidative stress analysis of AuNPs-corona complexes	page 9
Figure S9 Additional cryo-TEM images of AuNPs-corona complexes	page 9
References	page 10

Figure S1: Surface enhanced Raman spectroscopy (SERS) spectra of AuNPs without incubation in bovine serum (BS), and for comparison pure BS and fibrinogen (FIB). Note that bands in the spectrum of AuNPs can be assigned to the adsorption of phosphate anions from the stabilising buffer, onto the gold surface.¹

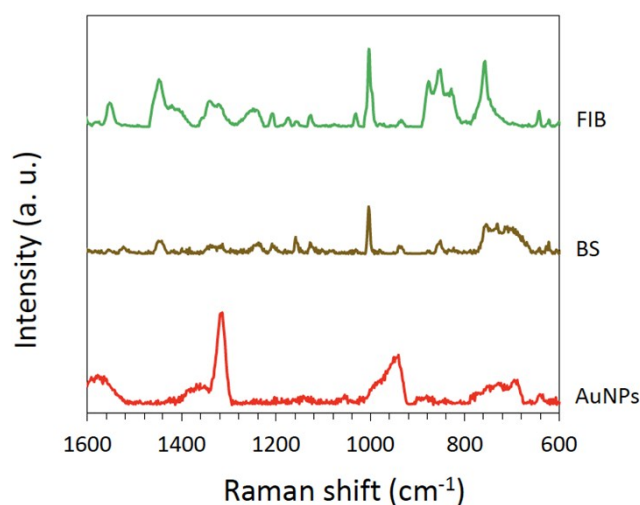


Table S1: Tentative assignments of Raman bands (excluding the free AuNPs).

Abbreviations: ν - stretching; δ - deformation; br - breathing; sym - symmetric; asym - asymmetric; wag - wagging; scis - scissoring; bend - bending; rock - rocking; tor - torsion; twist - twisting; R - C6 ring; r - C5 ring, iR - imidazole ring; Trp - tryptophan; Phe - phenylalanine; Pyr - pyrene; Tyr - tyrosine, Lys - lysine.

Au	BS	T ₁₀			T ₃₀			T ₁₂₀			Assignment and references
		W ₁	W ₂	W ₃	W ₁	W ₂	W ₃	W ₁	W ₂	W ₃	
1572	1571	1576	1569	1564	1570	1560	1559				iR (C=C, C=N) ν N τ -H bend, Trp ^{2,3}
	1553				1543	1533	1533				Amide II, Trp: ν (R, r) ⁴
	1523							1525			Tyr ⁵
	1448										asym δ (CH ₃), bend (CH ₂) ⁵
	1402										ν (CO-) ⁵
	1337										δ (CH); wag (CH ₂ , CH ₃) ⁴
1313	1317	1309	1308	1317	1313		1308				Wag (CH ₂), ⁵
						1291		1285	1291	1292	Twist (CH ₂) ⁶
	1238										Trp, Phe: δ (R) ^{2,5}
	1209										Tyr, Phe ²
	1159										ν (C-N) ²
	1127										ν (C-N, C-C) ²
	1072										ν (C α -N, C-CH ₂), bend (NH ₂), ν (C-O) ²
	1031					1028					Phe: in-plane ring CH δ ⁴
992	1004	1004	1004		999	1001	1000	1002	1001	1001	Phe: indole asym ring br ⁴
940	941	940	941	935	946	951	956	951	941	941	ν (C-C) ⁴
	897										R ²
	876							875			H (R, r) scis, N-H bend ²
	845	856	853	846	842			844	842	842	ν (C α -N, C-C), Tyr ²
	828										Tyr: δ (CCH) aliphatic, Tyr (ring) ⁶
	759										η (Pyr br), η 15 ⁴
689	698	711	693	700	694	678	678	689	684	683	COO- ³
	662						662				ν (C-S) ²
	643				639	648		641	641		Tyr: δ (R, CH), δ (C-S) ²
	622	613									R ν , R br ³

Figure S2: Comparison of proteomics data obtained from mass spectrometry analysis of AuNPs incubated in BS at different incubation times in minutes (T₁₀, T₃₀ and T₁₂₀). Analysis was conducted on the hard PC, whereby the samples underwent three washing cycles before trypsin digestion

(referred to as W_3). (a) Shows a comparison of detected proteins by function. (b) Venn diagram displaying the number of unique and common proteins identified in the coronas of the different samples.

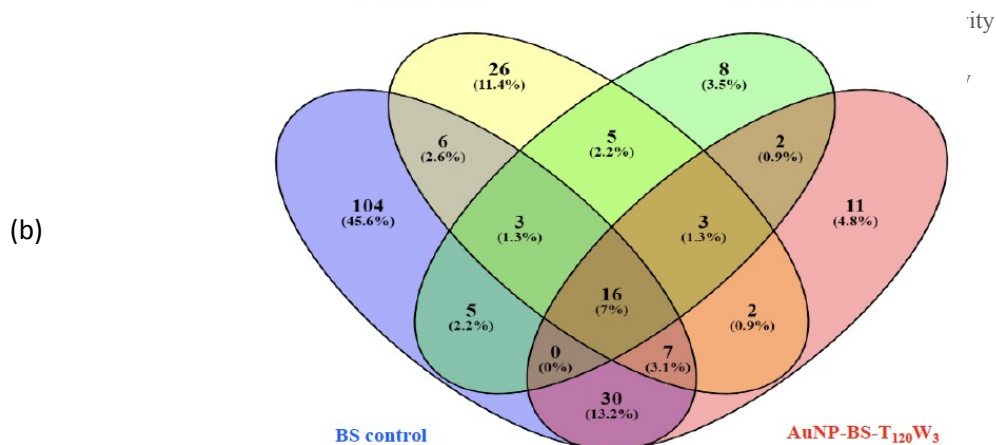
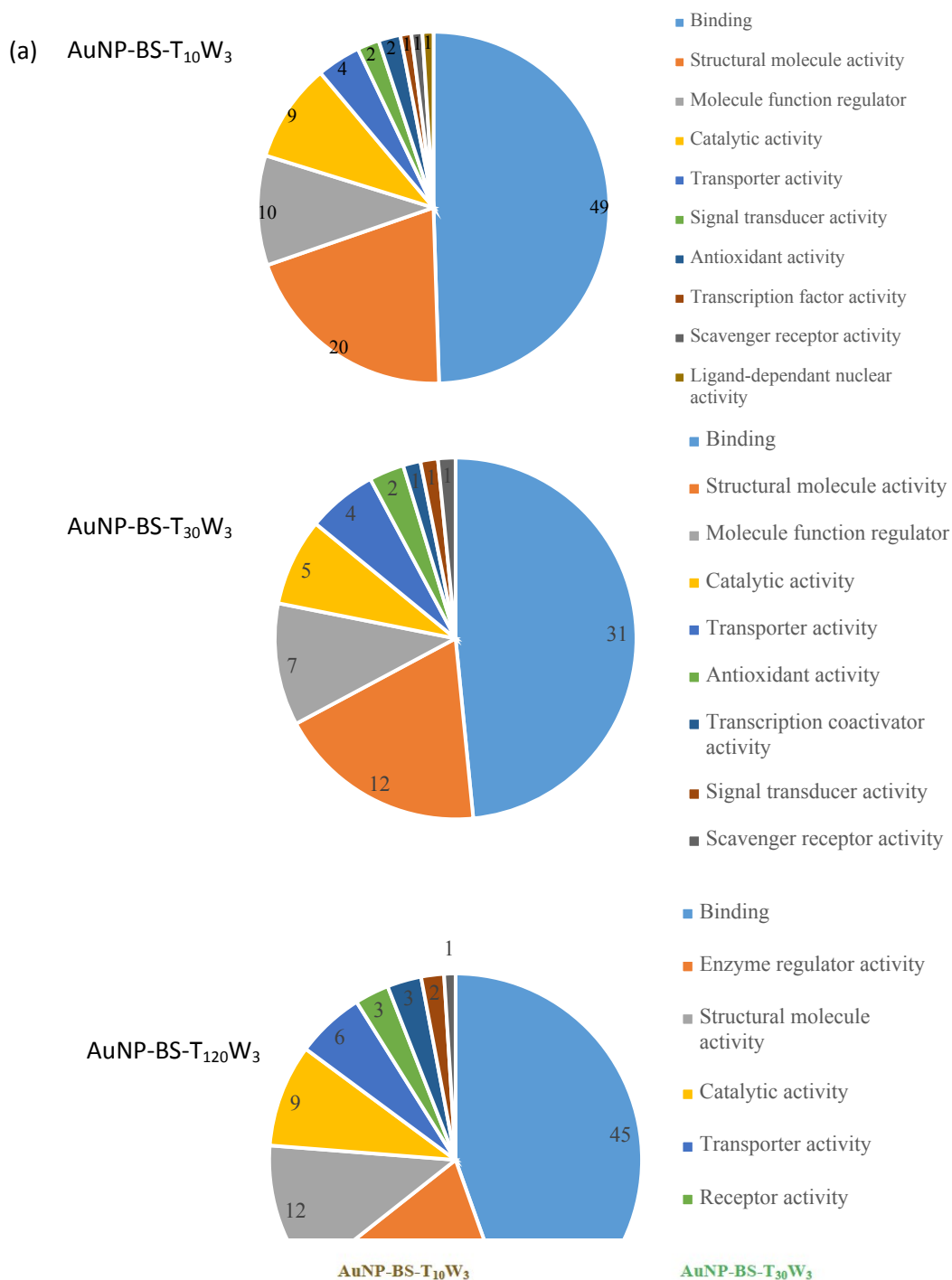


Table S2 Small Angle X-ray Scattering (SAXS) and results of the pair distance distribution function (PDDF) analysis using software ScÅtter.

For SAXS measurements AuNPs were dispersed in water at several concentrations of bovine serum (BS) and fibrinogen (FIB). The NP concentration was kept at 0.02mg/ml with BS and FIB concentrations of 0 (pure AuNPs), 0.25, 0.5, 2.5mg/ml. All experiments were performed at room temperature. Buffer curves (MilliQ water) were subtracted from the sample curves.

Prior to analysis, the SAXS measurement curves were averaged and background corrected, i.e. the buffer signal was subtracted. For the analysis of the SAXS measurements the Guinier Radius (R_g) was determined via Guinier peak analysis with the software ScÅtter (by Robert Rambo, Diamond Light Source, UK). Furthermore, the PDDF and the maximum distance between two particles (D_{max}) was determined using the same software. The conversion from reciprocal to real space was performed via a modification of the Moore function.⁷

All values in Å	0.02mg Au NPs	Fibrinogen with Au			Bovine serum with Au		
		0.25mg	0.5mg	2.5mg	0.25mg	0.5mg	2.5mg
R_g reciprocal	211.7	240.2	228.7	244.4	213.2	212.4	211
R_g real	192.7	185.5	191.6	185.4	198.8	193.8	192.6
D_{max}	570	520	546	550	581	590	570

With the model-independent information gained from the PDDF, the data was fitted using the software Igor Pro (WaveMetrics Inc., USA). The best fit was obtained for the form factor with a Gaussian distribution of a core-shell spheroid (**Fig. S2**) in a dilute system. We noticed that the used fit is not accurate for highest protein concentrations due to excessive agglomeration. The parameters obtained from fit are listed in **Table S3**.

Figure S3: Raw data SAXS curves.

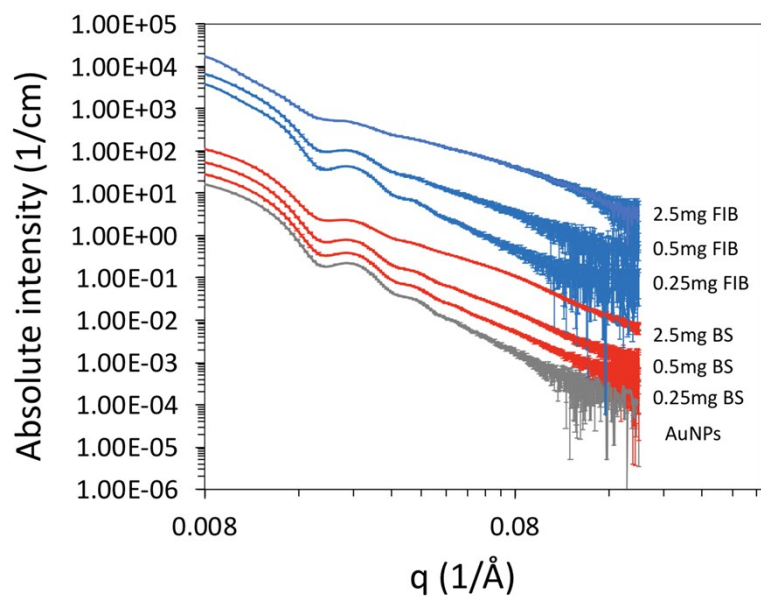


Table S3: Values obtained from the form factor fit of static SAXS data.

Sample	Core radius (Å)	Shell thickness (Å)
0.02mg/ml AuNPs	240.25	-
0.25mg/ml BS	248.1	18.04
0.5mg/ml BS	253.74	15.6
2.5mg/ml BS	272.5	16.19
0.25mg/ml FIB	245.38	31.75
0.5mg/ml FIB	268.88	10.61
2.5mg/ml FIB	308.76	4.09

Figure S4: Cryo-TEM images of (a) pure bovine serum (BS) showing amorphous dot-like contrast, (b) pure fibrinogen (FIB) showing a bent fibrous structure, and (c) pure FIB-BS showing structures similar to the BS image. The contrast of FIB-BS is slightly stronger than that of BS. Note that the shape of

fibrinogen is like a trinodular rod. The majority of the molecular weight is on the nodule part, not on the arm, making it hard to directly see the elongated fibrous structure under cryo-TEM.

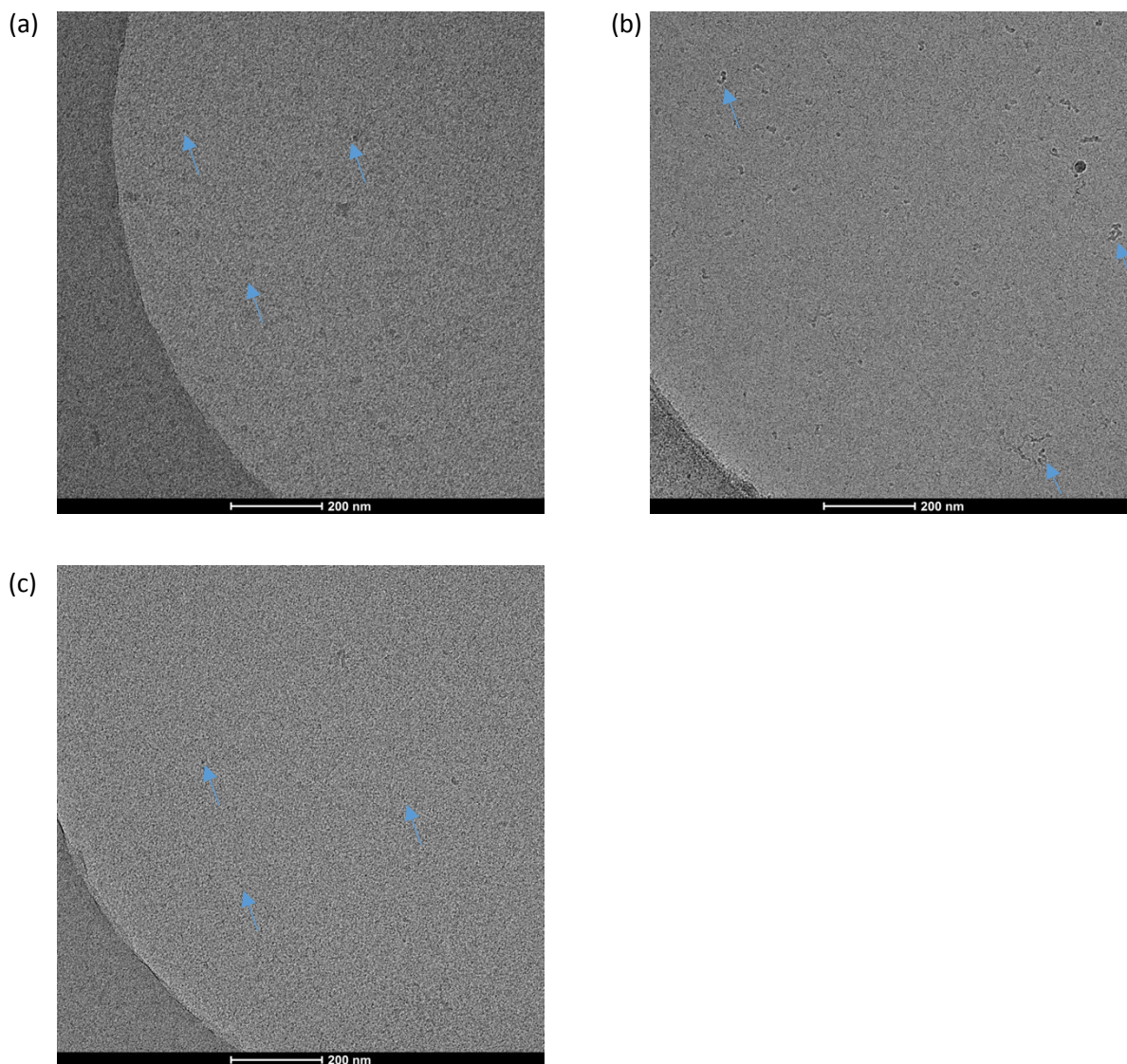


Figure S5: (a) DLS measurements of different AuNP-corona complexes in MilliQ water (W_{1-3}, T_{120}). (b) Zeta-potential measurements of different AuNP-corona complexes in MilliQ water.

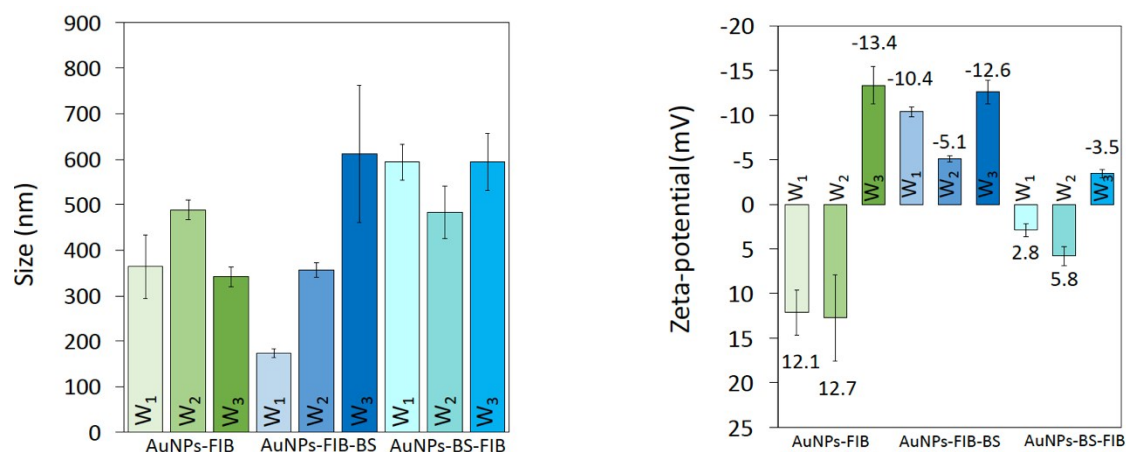


Figure S6: Biological TEM images visualising cell uptake of AuNP-corona complexes in microglia cells after 16 hours. (a) Pure cells (control) after 16 hours. (b) Pure AuNPs after 16 hours, cells show minor uptake. (c) Magnified image of cell uptake of pure AuNPs after 16 hours. (d) AuNP-BS-T₁₂₀W₃ corona complex, also minor cell uptake after 16 hours. (e) AuNP-FIB-T₁₂₀W₃ corona complex after 16 hours, no obvious cell uptake. Micrographs show some lipid droplets. (f) AuNP-FIB-BS-T₁₂₀W₃ corona complex after 16 hours showing minor cell uptake.

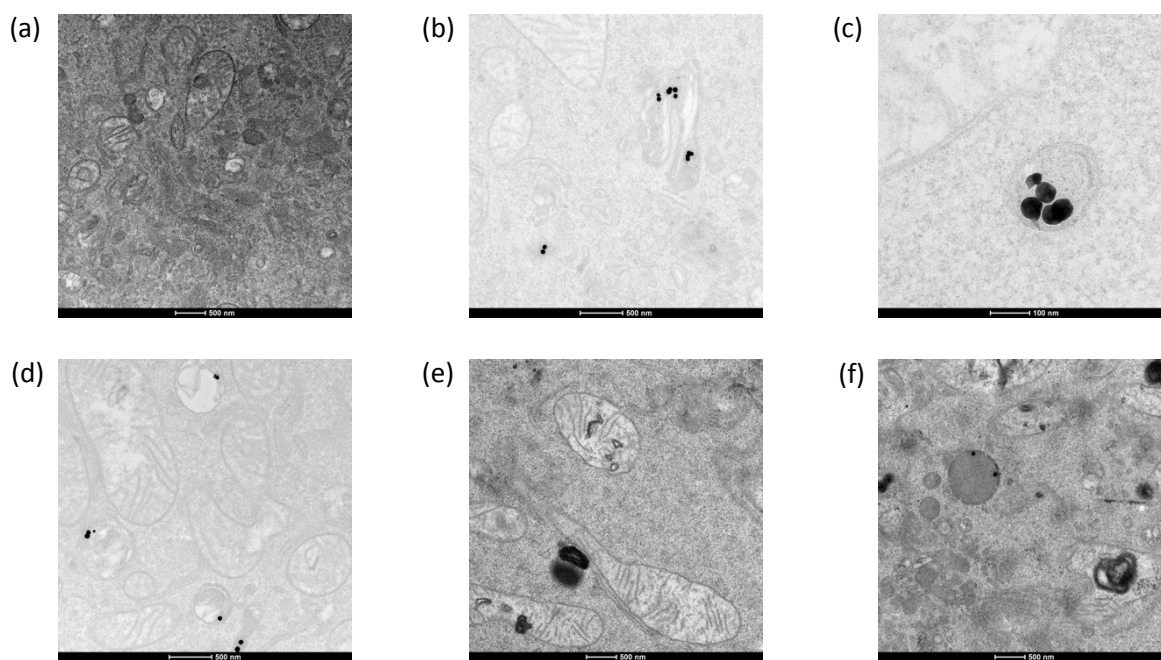


Figure S7: (a) Flow cytometry analysis of the cellular uptake of AuNPs with different corona complexes uptake by microglia after incubation for 16 (pattern bar) and 24 hours (solid bar) at 37°C. (b) Microglia under oxidative stress (ROS(+)) expressed as a percentage compared to normal cells

(ROS(-)) after 24 hours incubation, based on the intracellular detection of superoxide anion, when incubated with AuNPs with different corona complexes or with pure FIB or BS.

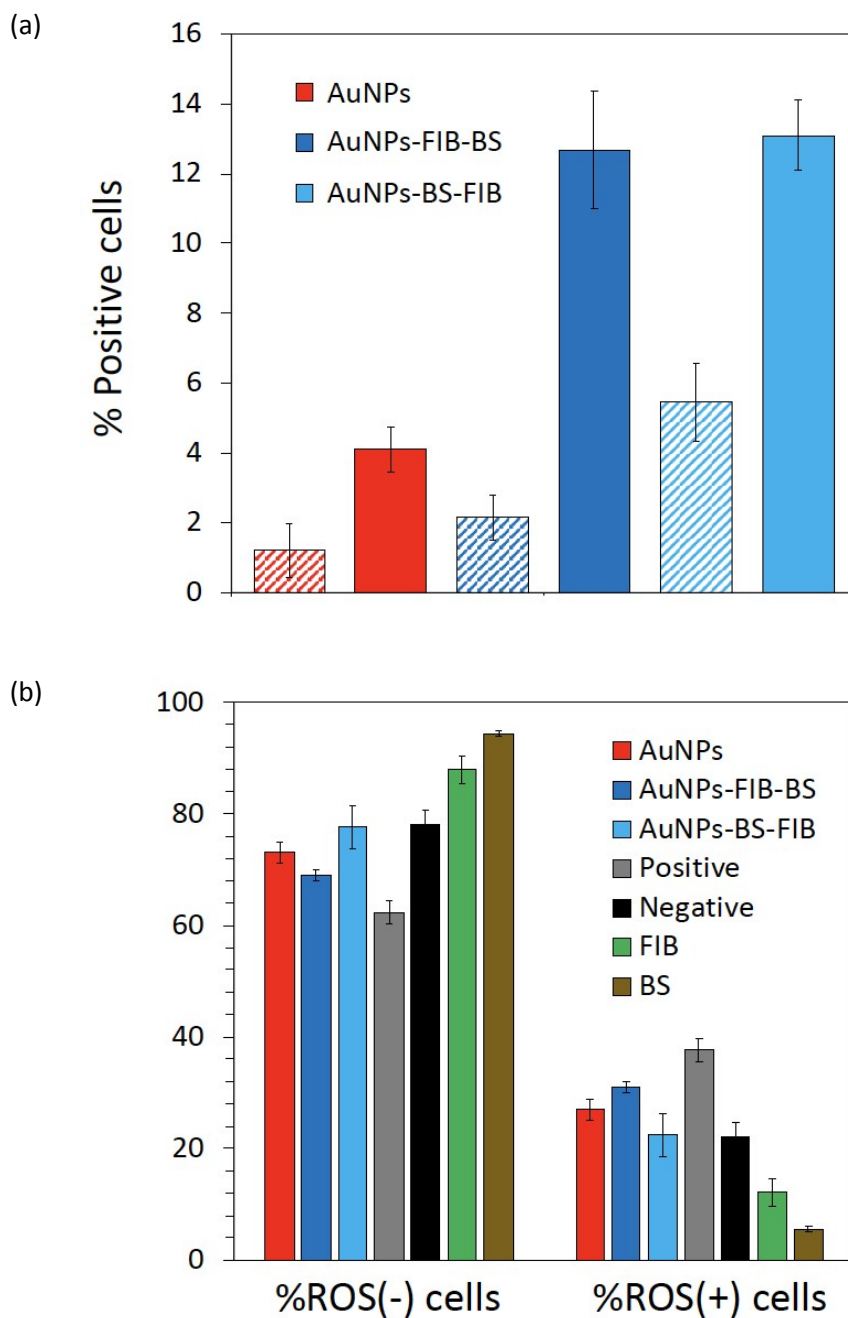


Figure S8: SERS spectra of hard PC of AuNP-corona complexes ($T_{120}W_3$) utilised for cell uptake studies. Pure fibrinogen (FIB) and bovine serum (BS) are included for comparison.

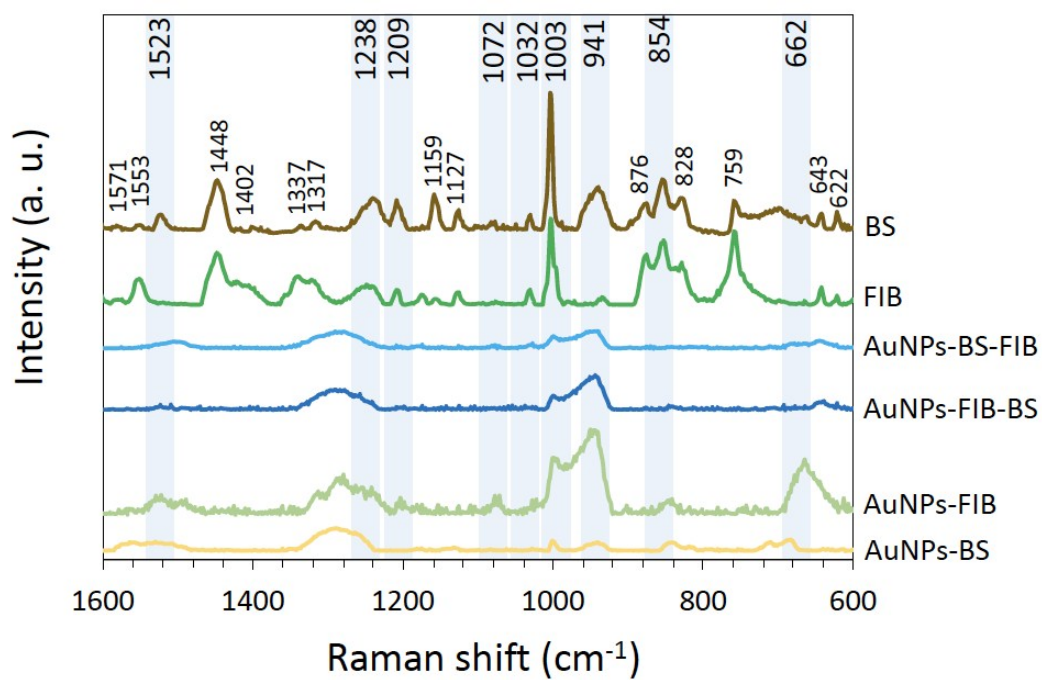
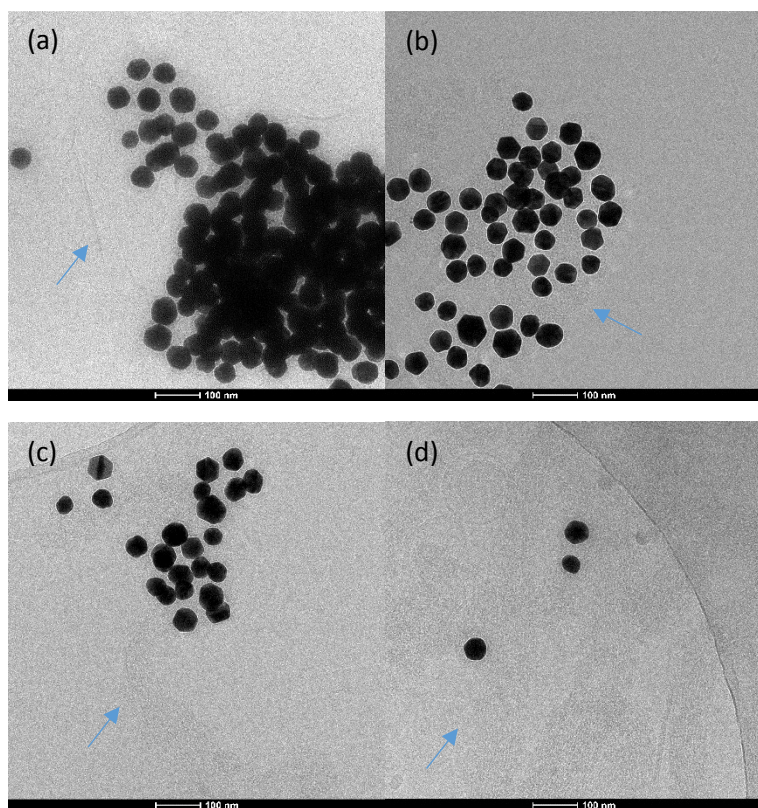


Figure S9: Additional cryo-TEM images of $T_{120}W_3$ -corona complexes of (a) AuNP-FIB (b) AuNP-BS and (c-d) AuNP-FIB-BS. Arrows show the formation of a PC and fibrous structures, showing a thicker fibrous PC for AuNP-FIB-BS than AuNP-FIB.



References:

Electronic Supporting Information

1. A. G. Miller and J. W. Macklin, *Analytical Chemistry*, 1983, **55**, 684-687.
2. G. P. Szekeres and J. Kneipp, *Frontiers in Chemistry*, 2019, **7**.
3. F. Madzharova, Z. Heiner and J. Kneipp, *The Journal of Physical Chemistry C*, 2017, **121**, 1235-1242.
4. D. Drescher, T. Büchner, D. McNaughton and J. Kneipp, *Physical Chemistry Chemical Physics*, 2013, **15**, 5364-5373.
5. S. Barkur and S. Chidangil, *Journal of Biomolecular Structure and Dynamics*, 2019, **37**, 1090-1098.
6. J. Kneipp, H. Kneipp, B. Wittig and K. Kneipp, *Nanomedicine: Nanotechnology, Biology and Medicine*, 2010, **6**, 214-226.
7. I. Pilz, O. Glatter and O. Kratky, *Methods Enzymol*, 1979, **61**, 148-249.